LTE-BASED SCALABLE DRONE COMMUNICATION: FLIGHT TEST RESULTS FROM AN URBAN U-SPACE LIKE OPERATION

F. Frickenstein*, B. Lochow*, T. Piechotta†‡, A. Finn †, M. Rossol§, C. Janke¶, M. Uijt De Haag*

* Technische Universität Berlin, Fachgebiet Flugführung und Luftverkehr, Marchstraße 12-14, Berlin, Germany
† Fraunhofer-Institut für Nachrichtentechnik, Heinrich-Hertz-Institut, Einsteinufer 37, Berlin, Germany
‡ Flybionic UG, Nuthestraße 39c, Berlin, Germany
§ b.r.m. IT & Aerospace GmbH, Schwachhauser Heerstraße 214, Bremen, Germany
¶ Embry-Riddle Aeronautical University, Worldwide Campus, Germany

Abstract

The increasing use of Uncrewed Aerial Vehicles (UAVs) for tasks in urban environments during recent years has driven the need for reliable communication systems and precise relative positioning capabilities. The mFund project SKADRO (Scalable Drone Communication Systems for U-space areas) aims to tackle reliable UAV communication by utilizing LTE, particularly in low-level airspace and U-Space, addressing challenges such as cellular network congestion and the effects of urban infrastructure on signal propagation. The latter also affects the accuracy of Global Navigation Satellite Systems (GNSS) used for absolute and relative positioning, and effects include multipath effects, non-line-of-sight propagation or shadowing.

This paper presents results from a flight test that has been conducted at the Technische Universität Berlin, where three UAVs were operated under U-space conditions. The UAVs were equipped with a custom sensor payload consisting of a 4G/5G communication device developed during the mFund project SUCOM (Superior UTM Communication System), a camera, and a custom sensor box consisting of a GNSS receiver, a Software-Defined Radio, an ADS-B transceiver, an Ultrawide-band Radio, and a laser altimeter. During this test, the U-space Service Provider (USSP) b.r.m. IT & Aerospace provided a recognized air picture based on ADS-B, which is compared to the position information transmitted through the cellular network. Real-time data, including video streams, were transmitted to Fraunhofer Heinrich-Hertz-Institute's TimeLab for real-time monitoring and analysis of beyond-visual-line-of-sight (BVLOS) capabilities of the UAV operations within the U-space environment.

In addition to vehicle-to-infrastructure (V2I) communication, the study explores the feasibility of direct vehicle-to-vehicle (V2V) communication using the Automatic Dependent Surveillance - Light (ADS-L) as proposed by the European Union Aviation Safety Agency (EASA). While this standard utilizes the short-range 860 (SRD-860) frequency band, rather a version transmitted over the cellular network is used. The findings highlight the potential advantages of V2V communication in urban environments, where direct communication between UAVs might enhance operational reliability and safety.

1. INTRODUCTION

With the rapid expansion of uncrewed aerial vehicles (UAVs) in civilian airspace for applications ranging from emergency response and traffic monitoring to infrastructure inspection and time-critical delivery of medical goods, the operational complexity of lower airspace, particularly in urban environments, is expected to grow.

To enable the safe operation of UAVs in such environments and to ensure effective coordination with crewed aviation, the European Union Aviation Safety Agency (EASA) has introduced the concept of U-space, defined as a set of services provided in an airspace volume designated by the Member State to manage a large number of UAS operations in a safe and efficient manner [2].

A key challenge of integrating UAVs into urban and very low-level (VLL) airspace is the simultaneous coordination of multiple UAV operations. To support safe and efficient operations at scale, U-space services such as communication, airspace monitoring, and separation assurance are required to ensure collision-free and reliable mission execution.

Systems have been implemented to address these challenges under realistic conditions, and this paper presents results from a flight test conducted at the North-campus of Technische Universität Berlin (TU Berlin) within an experimental U-space trial (U-space tr) environment. In this test, b.r.m. IT & Aerospace GmbH acted as the U-space Service Provider (USSP), while the TimeLab at Fraunhofer Heinrich-Hertz-Institut operated a beyond visual line-of-sight (BVLOS) control center and the TU Berlin as UAV operator.

The primary objective of the test was to assess different possible communication lines between all U-

doi: 10.25967/650218

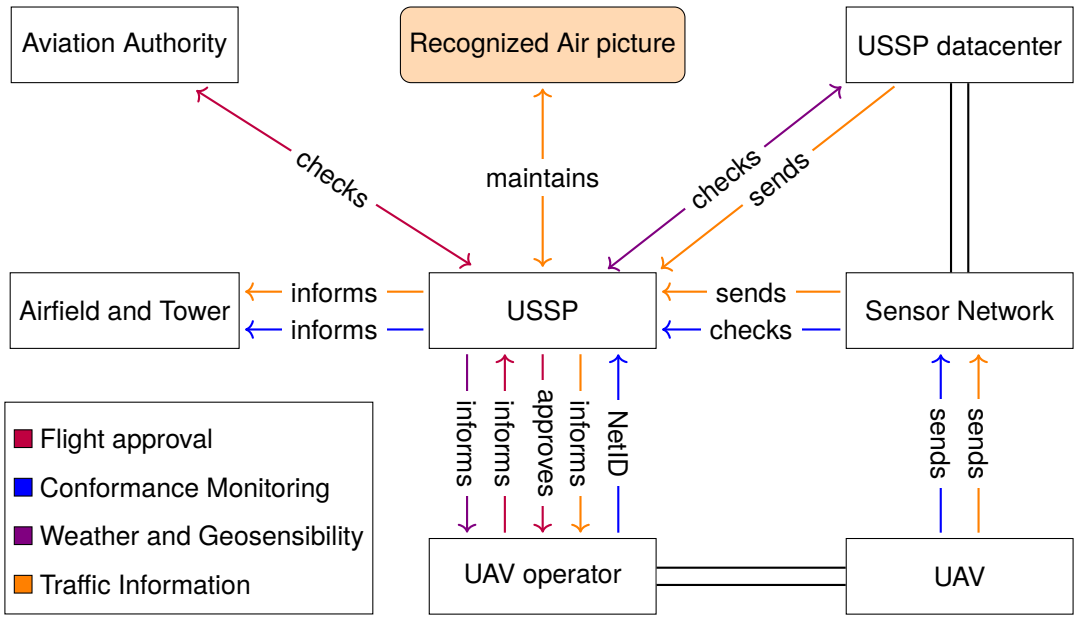

FIG 1. U-space entities and the services connecting them [1]

space stakeholders, with a particular focus on LTE-based communication solutions.
In addition to verifying compliance with current regulations, measurement data was collected to evaluate the performance of different visibility and surveillance methods, including Automatic Dependent SurveillanceBroadcast (ADS-B), Automatic Dependent SurveillanceLight (ADS-L), and a modified ADS-L message format transmitted via LTE. The latter format takes advantage of the benefits of using raw GNSS data for relative navigation. To assess the influence of urban infrastructure on these systems, comparable flight scenarios using the same equipment were carried out in an open field near Baruth/Mark 24 days later.
The remainder of this paper is structured as follows. Section 2 provides the regulatory background on U-space. Section 3 describes the communication links and protocols employed during the test. Section 4 details the experimental setup, including the flight test areas and UAV fleet. Section 5 presents and discusses the findings of the test. Finally, Section 6 concludes the paper and outlines potential directions for future research.

2. U-SPACE

In this section, a concise overview of the implemented U-space services is provided. A more comprehensive discussion can be found in [1]. U-space services, as defined in the Commission Implementing Regulation (EU) 2021/664 " a regulatory framework for U-space" of 22 April 2021 [2], can be categorized into four groups that interconnect the following entities:

- the national aviation authority,
- the USSP and the associated USSP data center,
- the Common Information Service Provider (CISP), and
- the UAV operator with its aircraft platform(s).

The *flight approval service* is triggered when the UAV operator submits a flight plan to the USSP prior to mission execution. The USSP then verifies compliance with applicable requirements for both the UAV and the operator, and assesses potential conflicts with other flight plans. Once approval is granted, the corresponding flight status is made available to other relevant airspace stakeholders.
The *network identification and conformance monitoring* services cross-reference telemetry data with a unique network identifier (*NetID*, e.g., a hexadecimal code) to track the missions adherence to the approved flight plan. The resulting conformance information is made accessible to other stakeholders.
The *weather and geo-awareness* service consists of the USSP acquiring current meteorological data and information on airspace constraints. This includes temporary no-fly zones, geofencing information, and continuous weather monitoring.
The *traffic information service* provides and maintains a recognized air picture generated by fusing data from multiple sources, such as ground-based sensors and information broadcast by cooperative UAVs. This recognized air picture is continuously shared with all relevant stakeholders, in particular UAV operators, to enable real-time decision-making in the event of potential conflicts.
An overview of these services and their interconnections with the respective entities is presented in Figure 1.

3. COMMUNICATION AND PROTOCOLS

For U-space services it is necessary that UAVs operating the the service volume remain continuously observable to the USSP and aware of each other. This is especially important for the recognized air picture and

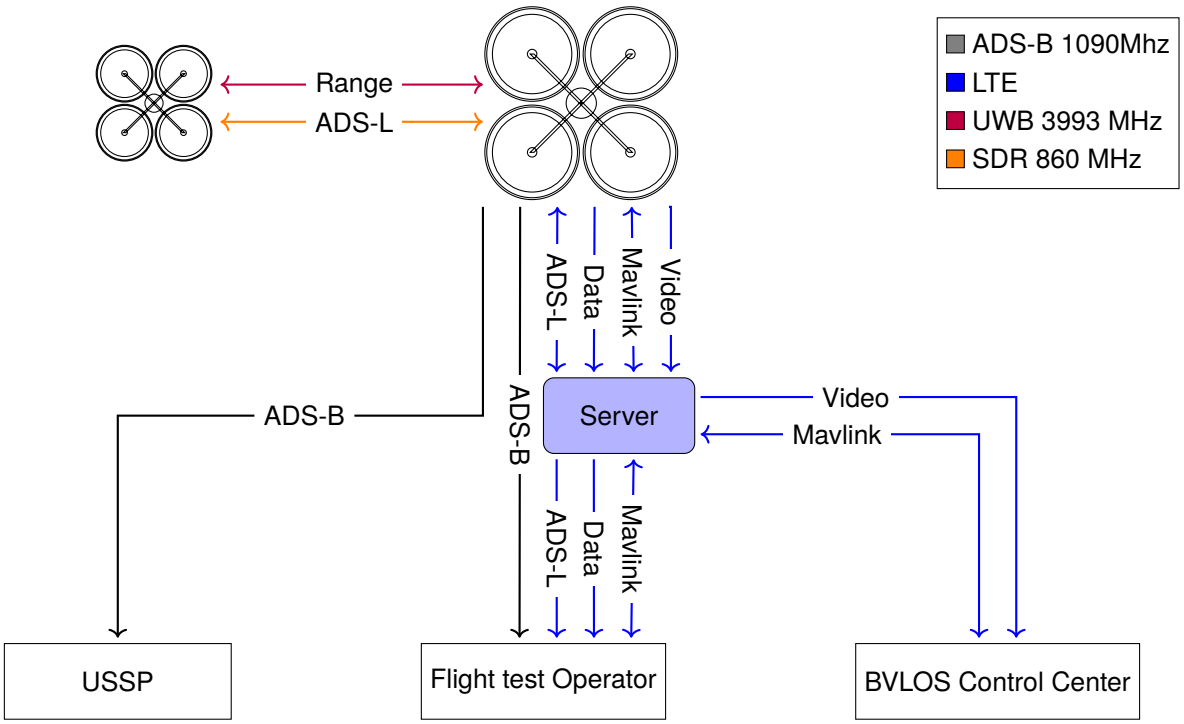

FIG 2. The projects communication infrastructure.

surveillance functions required to operate effectively and safely. This section describes the communication methods that were evaluated during the flight test campaign.

3.1. Automatic Dependent Surveillance - Broadcast

Automatic Dependent SurveillanceBroadcast (ADS-B), while well established, is not mandatory in European airspace for aircraft with a maximum take-off mass below 5.7 metric tons [3]. ADS-B messages are transmitted either via a Mode S transponder operating at 1090 MHz or via a *Universal Access Transceiver* (UAT) operating at 978 MHz [4]. The latter method is, however, not available in Europe.
Each ADS-B message has a total length of 112 bits, of which 56 bits are allocated to the message-specific payload. This payload encodes, among other parameters, surveillance status, barometric altitude, time information, as well as latitude and longitude and velocity estimates, enabling future loss-of-separation estimations. A total of 17 bits are dedicated to the encoding of latitude and 17 bits to the encoding of longitude, which enables a horizontal positional accuracy of approximately 5 meters due to the use of the *Compact Position Reporting* (CPR) encoding.
The CPR format requires two consecutive messages (one odd frame and one even frame) or a known reference position in order to reconstruct the position of the aircraft unambiguously.

3.2. Automatic Dependent Surveillance - Light

To address the need for a standardized surveillance solution for aircraft with a maximum take-off mass below 5.7 tons in Europe, the EASA introduced *Automatic Dependent SurveillanceLight* (ADS-L) in 2022 [5], which has since been revised in 2025 [6]. In contrast to ADS-B, ADS-L requires only a single message without CPR encoding and reserves 120 bits for the message-specific payload. Of these, 24 bits are assigned to each latitude and longitude, yielding a resolution of approximately 1.2 meters. The EASA ADS-L standard describes two physical layer transmission options in the 860MHz band. One of these has been implemented using software-defined radios operating in the 860 MHz band. In addition, a separate ADS-L implementation is envisioned via LTE.
It should be noted that both ADS-B and ADS-L may introduce resolution-induced errors when used for relative positioning between aircraft.

3.3. Adjusted ADS-L with raw GNSS data

In contrast to approaches based on absolute positioning, a method that uses pseudo-ranges and carrier-phase measurements for relative navigation was developed and validated in [7]. Based on this work, an adapted ADS-L message format was proposed in [8]. In this method, raw GNSS data is transmitted and subsequently processed using triple differencing techniques and error compensation in order to directly estimate the baseline vector, that is, the relative position vector, between two aircraft from (carrier-smoothed-code) pseudorange measurements, as well as the baseline change vector, that is, the relative velocity vector, from carrier-phase measurements. Due to its elevated bandwidth requirements, the method is designed for transmission over LTE.

By restricting the processing to satellites that are commonly observed by both platforms, it becomes possible to directly determine the relative position and relative velocity while canceling common errors. This yields a solution with higher accuracy and integrity than relative positioning based on ADS-B or conventional ADS-L.
Table 1 gives an overview of the different protocols.

3.4. Further surveillance communication links

In addition to the systems presented above, all protocols (with the exception of ADS-B) are transmitted via an LTE connection to a centralized server and subsequently relayed to the UAV (flight test) operator. Furthermore, a bidirectional communication link is established between the flight controller, the BVLOS control center, and the flight test operator.
This communication link contains information on the position, trajectory and operational status of the UAV, which allows real-time monitoring and adjustment of flight paths. In addition, a video data stream is transmitted to the control center to enable BVLOS operations conducted by a remote pilot.
All UAVs are furthermore equipped with an ultra-wideband (UWB) radio system operating at 3993 MHz, which is used to make range measurement between the various UAV platforms. The range measurements can be used in addition to the position and velocity reports from ADS-B or ADS-L for collision detection and conformance monitoring purposes.
Figure 2 shows a diagram of the communication infrastructure of the project.

4. FLIGHT TEST SETUP

4.1. Fleet

Three Holybro X500v2 quadcopters, each equipped with a custom sensor payload, were deployed for the flight experiments. The payload configuration consisted of a GNSS receiver based on a Septentrio Mosaic X5 module, an ESP32-based ultra-wideband (UWB) radio, a Benewake TF03 laser altimeter, an Aerobits TR1F ADSB transceiver with an independent GNSS antenna, and a USRP B205minii software-defined radio (SDR). Furthermore, all UAVs were equipped with an LTE communication module that was specifically adapted and optimized for the requirements of this project. Two of the three platforms were additionally equipped with a camera system.
An exploded view of the UAVs utilized in this study is presented in Figure 3, and the assembled UAVs are depicted in Figure 4. ADS-B position data was collected both by fixed infrastructure distributed around the city and by a local on-site receiver. For the GNSS reference data, the position estimates provided by the Septentrio Mosaic X5 receiver were used, although without the application of Real-Time Kinematic (RTK) corrections.

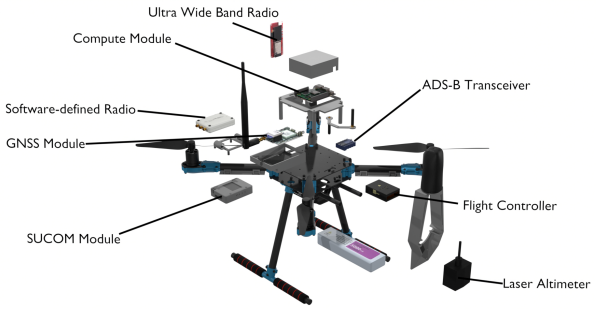

FIG 3. Exploded view of the setup of each UAV.

FIG 4. The fleet used in the project.

4.2. Locations

The primary flight test was conducted at the North campus of Technische Universität Berlin and forms part of a broader sequence of flight experiments within the project SKADRO [9]. The approved test area covers approximately 150 m by 200 m and lies within ED-R 146, the restricted airspace around the German Bundestag.
To ensure operational safety, access control measures were implemented by temporarily closing all relevant entry and exit points to the ground area during flight operations. All flights were conducted strictly under visual line-of-sight (VLOS) conditions and no temporary restriction or closure of the airspace itself was enacted.
In addition to the applicable official regulations, supplementary self-imposed operational constraints were defined. These included a maximum flight altitude of 75 m above ground level and a further reduction of the practically used flight area for additional safety. A visualization of the approved flight area, the contingency regions, and the closed access points is depicted in Fig. 5.
For the purpose of obtaining comparable measurement data, similar trajectories were replicated with the same equipment in an open-field environment near Baruth/Mark on Tuesday 19th August, 2025.

Protocol	Transmission	Payload	Resolution	Note
ADS-B	1090 MHz/978 MHz	56 bit	~ 5 m	CPR encoded
ADS-L	860 MHz	120 bit	~ 1.2 m	
ADS-L raw	LTE	arbitrary (>120 bit)	< 1 m	Relative poisitioning only

TAB 1. Comparison of the different communication protocols.

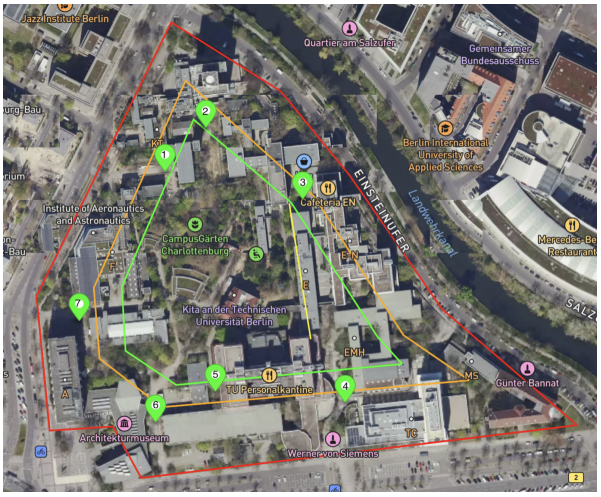

FIG 5. North-campus of Technische Universität Berlin showing the approved safety and contingency areas. The yellow line denotes the self-imposed limitation of the operational airspace, and the numbered markers indicate the seven relevant ground access points to the area.

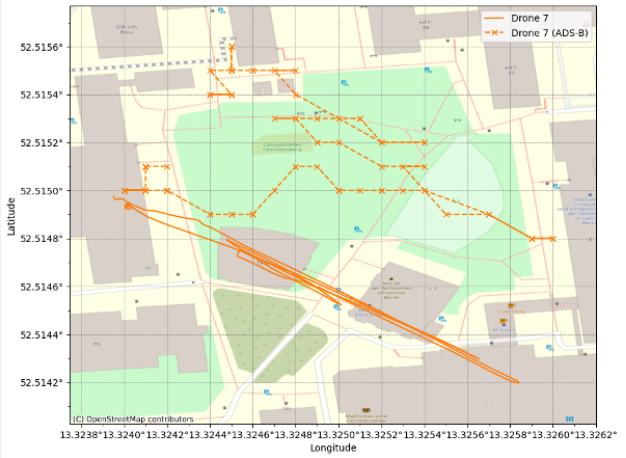

FIG 7. Locally recorded ADS-B position of Drone 7 (dashed) and corresponding recorded ground-truth trajectory (solid).

5. FLIGHT TEST RESULTS

The urban flight test was conducted over a three-hour period in the morning of Saturday 26th July, 2025. Operational constraints were due to written examinations being held on campus as well as a major public event in Berlin, both of which significantly restricted the available flight window. Figure 6 depicts Drone 7 and Drone 8 during take-off.

Two of the planned test flights could be completed successfully with a flight time of approximately four to five minutes, although ensuring sufficient visibility of ADS-B posed a major challenge. On the one hand, a significant offset was observed between the transmitted ADS-B position and the actual position, with deviations of up to $74.5\,\mathrm{m}$ East and $60.8\,\mathrm{m}$ North, and mean deviations of $41.2\,\mathrm{m}$ and $34.9\,\mathrm{m}$, respectively. The locally recorded ADS-B track of Drone 7 is shown in Figure 7.

FIG 6. The projects Drone 7 and Drone 8 during take-off at Technische Universität Berlin North-campus.

In addition, surrounding buildings temporarily obstructed the line-of-sight between the ADS-B transceiver and the fixed ADS-B ground reference stations receiving antenna, thus hindering continuous monitoring. Figure 8 presents the recordings of the fixed-infrastructure ADS-B system for Drone 7 and Drone 8. The shorter flight duration of Drone 8 (yellow) is clearly visible.

The flight tests conducted with the same fleet in Baruth/Mark on Tuesday 19th August, 2025 did not show comparable behavior, further highlighting the influence of urban environment on ADS-B performance with regards to the GNSS reception issues of the ADS-B module itself, as well as the lack of reception by the ADS-B ground stations. Figure 9 shows the locally recorded ADS-B position for Drone 7 (red) together with the ground-truth trajectory (orange).

Furthermore, it was possible to transmit and receive ADS-L data in the $860\,\mathrm{MHz}$ band in accordance with the initial EASA standard ([5]) in both locations. However, only 28% of the transmitted messages were successfully received via this channel, which might be due to the congested frequency and simple implementation. By contrast, all messages were reliably received via the LTE communication link. Figure 10 visualizes the deviation between the transmitted ADS-L position

FIG 8. Recordings of the fixed-infrastructure ADS-B system for Drone 7 (orange) and Drone 8 (yellow), showing a pronounced drift for Drone 7 and only a 30 s recording interval for Drone 8.

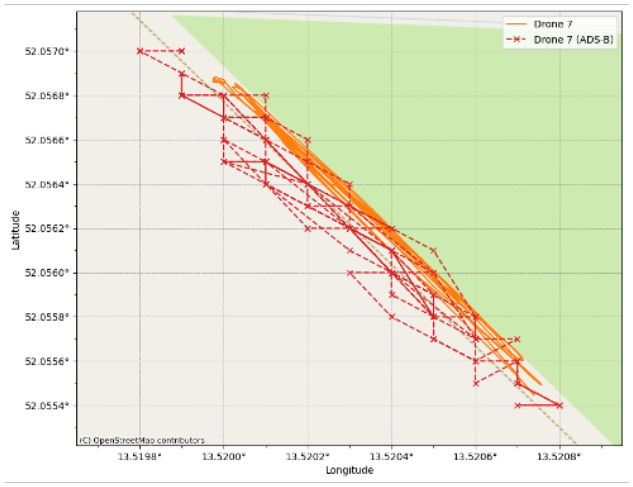

FIG 9. Locally recorded ADS-B data for the comparison flight in Baruth/Mark for Drone 7 (red) and the corresponding recorded ground-truth trajectory (orange).

FIG 10. Temporal evolution of the positional error between the transmitted ADS-L position and the recorded ground truth for Drone 1 and Drone 7.

and the recorded ground truth, which matches the expected resolution.

Throughout the entire operation, a continuous video stream with a resolution of 1280×720 at 30 frames per second and a throughput of 800 kilobytes per second, as well as vehicle status data in the mavlink format was successfully transmitted via LTE to both the BVLOS control center and the operator for real-time monitoring and supervision.

For the relative positioning methods based on raw GNSS observations, distinct differences in performance were identified between the urban and rural comparison flights.

In the urban scenario, relative positioning derived from pseudorange measurements between Drone 1 and Drone 7 yielded a mean deviation of $0.464\,\mathrm{m}$ in longitude and $0.511\,\mathrm{m}$ in latitude, with corresponding standard deviations of $0.987\,\mathrm{m}$ and $0.708\,\mathrm{m}$, respectively. When using the cumulative relative delta position estimates, corrected for the initial position, the mean deviation was reduced to $0.345\,\mathrm{m}$ in longitude with a standard deviation of $0.826\,\mathrm{m}$, and to $0.708\,\mathrm{m}$ in latitude with a standard deviation of $0.752\,\mathrm{m}$. This indicates a marginal improvement in accuracy compared to the use of pseudorange-based positioning alone. The comparison of the relative positions in the east and north directions is presented in Figures 11 and 12, respectively. A graphical representation of the resulting position deviations (deltas) is provided in Figures 13 and 14.

In the corresponding experiment conducted in the open-field environment near Baruth/Mark, relative positioning based on pseudorange measurements resulted in a mean deviation of $0.098\,\mathrm{m}$ in longitude and $0.290\,\mathrm{m}$ in latitude, with standard deviations of $0.290\,\mathrm{m}$ and $0.353\,\mathrm{m}$, respectively. In this setting, the cumulative relative delta positioning produced a mean deviation of $0.625\,\mathrm{m}$ in longitude with a standard deviation of $0.386\,\mathrm{m}$, and a mean deviation of $0.835\,\mathrm{m}$ in latitude with a standard deviation of $1.01\,\mathrm{m}$. The relative displacements in the eastward and northward

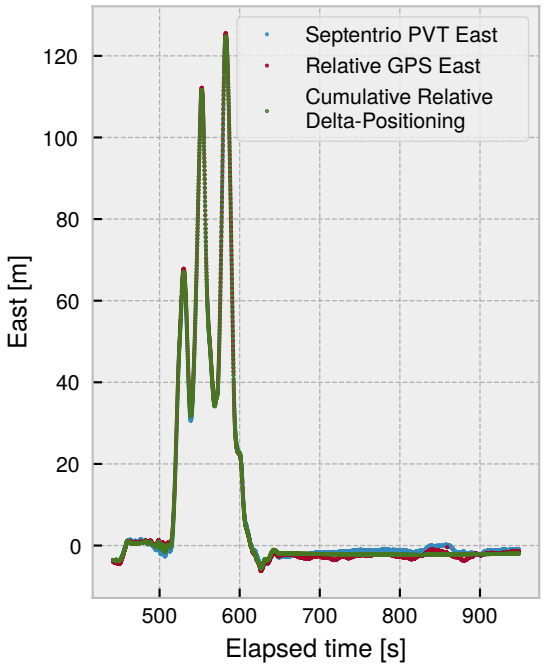

FIG 11. Comparison of the relative position in the eastward direction for the urban environment derived from the recorded ground-truth data (blue), the pseudorange-based relative position (red), and the relative position obtained from the cumulative relative velocities between Drone 1 and Drone 7 (green).

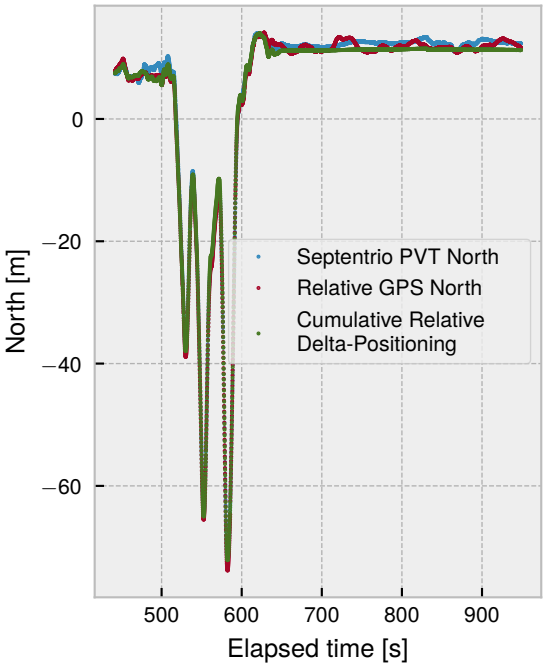

FIG 12. Comparison of the relative position in the northward direction for the urban environment derived from the recorded ground-truth data (blue), the pseudorange-based relative position (red), and the relative position obtained from the cumulative relative velocities between Drone 1 and Drone 7 (green).

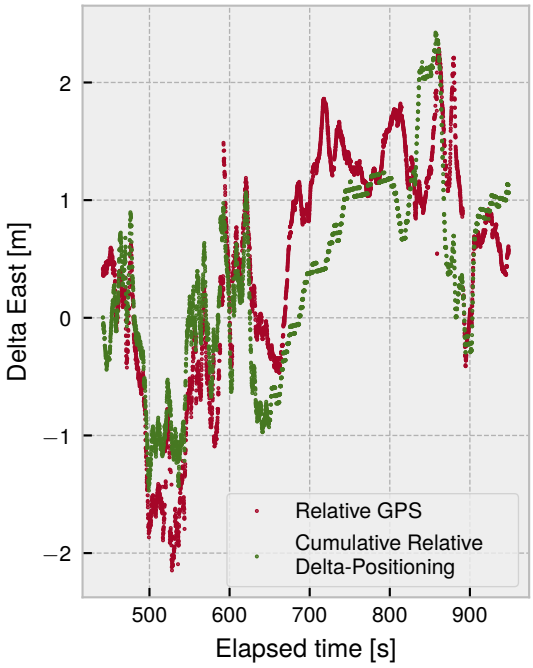

FIG 13. Longitude difference between Drone 1 and Drone 7 in the urban environment, comparing the relative position derived from pseudorange measurements (red) with the ground truth, and the cumulative delta relative position estimate obtained from relative velocity estimates based on pseudorange and carrier-phase measurements (green).

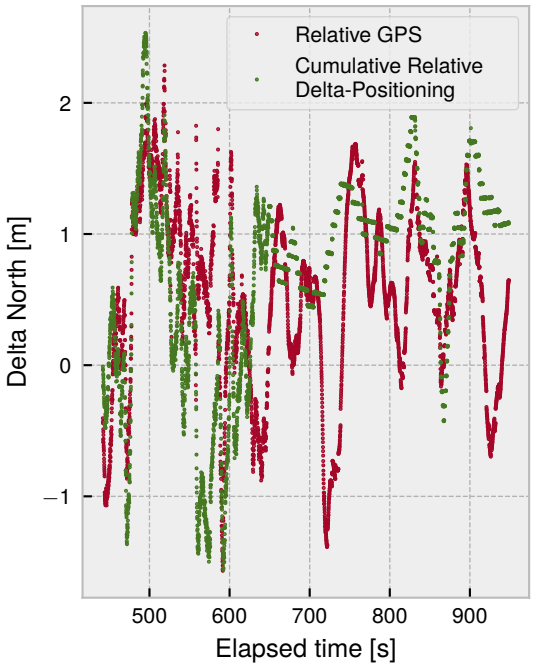

FIG 14. Latitude difference between Drone 1 and Drone 7 in the urban environment, comparing the relative position derived from pseudorange measurements (red) with the ground truth, and the cumulative delta relative position estimate obtained from relative velocity estimates based on pseudorange and carrier-phase measurements (green).

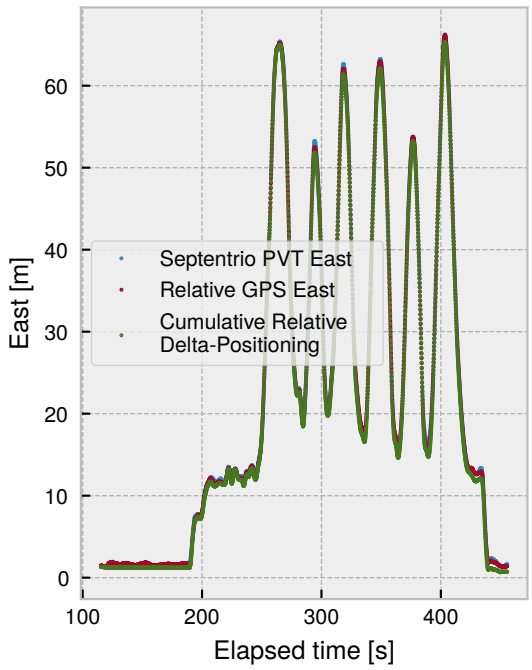

FIG 15. Comparison of the relative position in the eastward direction for the rural environment derived from the recorded ground-truth data (blue), the pseudorange-based relative position (red), and the relative position obtained from the cumulative relative velocities between Drone 1 and Drone 7 (green).

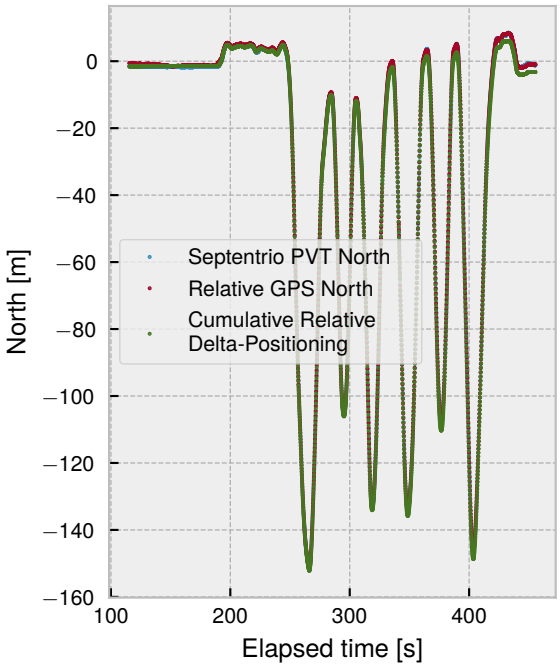

FIG 16. Comparison of the relative position in the northward direction for the rural environment derived from the recorded ground-truth data (blue), the pseudorange-based relative position (red), and the relative position obtained from the cumulative relative velocities between Drone 1 and Drone 7 (green).

directions are presented in Figure 15 and Figure 16. The corresponding deviations are depicted in Figure 17 for longitude and in Figure 18 for the latitude component.

In this rural scenario, the purely pseudorange-based method provides slightly superior accuracy, further emphasizing the conceptual and performance differences between open-field and urban environments.

Note that no additional filtering or smoothing was applied to the GNSS-based estimates. Furthermore, the ground-truth reference solution is uncorrected and therefore exhibits a worst-case absolute accuracy on the order of approximately $1.2\,\mathrm{m}$ [10].

6. CONCLUSION AND OUTLOOK

The paper presents preliminary results from a flight test campaign involving multiple UAVs in an urban environment under U-space conditions. The findings demonstrate that the implemented U-space services are operational, although they also highlight a considerable potential for further optimization.

A persistent challenge concerns the reliable visibility and situational awareness of all participants, particularly in dense urban settings. In such environments, the existing ADS-B infrastructure can be subject to signal obstruction caused by buildings, and the EASA ADS-L standard is still in an early stage of development and requires further maturation.

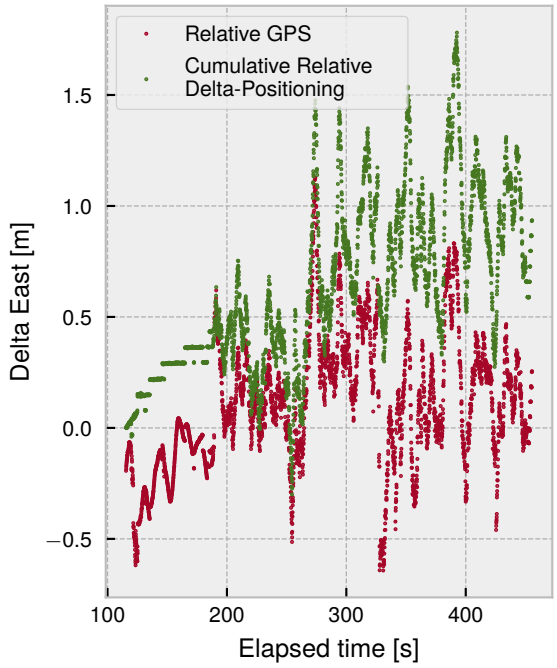

FIG 17. Longitude difference between Drone 1 and Drone 7 in the rural environment, comparing the relative position derived from pseudorange measurements (red) with the ground truth, and the cumulative delta relative position estimate obtained from relative velocity estimates based on pseudorange and carrier-phase measurements (green).

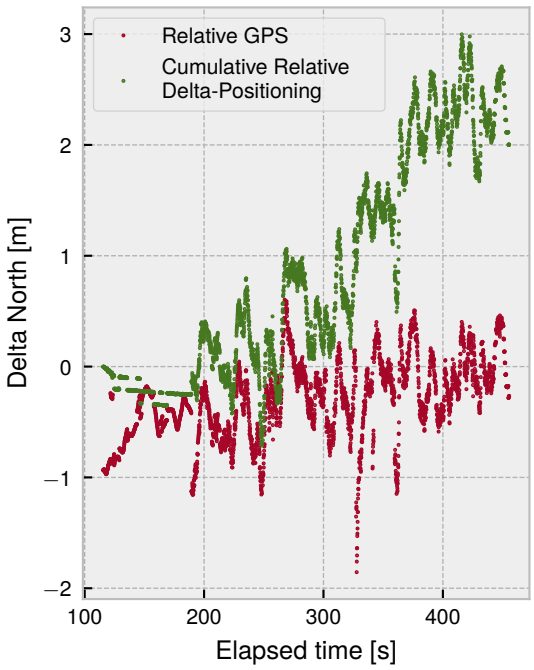

FIG 18. Latitude difference between Drone 1 and Drone 7 in the rural environment, comparing the relative position derived from pseudorange measurements (red) with the ground truth, and the cumulative delta relative position estimate obtained from relative velocity estimates based on pseudorange and carrier-phase measurements (green).

The study provides evidence that LTE-based communication constitutes a viable solution, and that the increased available bandwidth can be effectively utilized for the transmission of range-based measurements.
The differences observed between the urban and rural test environments suggest several directions for future research, particularly with respect to the filtering of raw sensor data. In addition, they open up further investigation of fused approaches that combine fixed-position solutions with partial raw measurements to enable smoothing and correction, thereby bridging the gap between relative and global positioning.
Furthermore, the method based on raw GNSS measurements can be applied for conformance monitoring in scenarios where the intended trajectory is known, for instance within a message structure of the type proposed in [11].
Future work will comprise a flight test campaign including both UAVs and small manned aircraft, all equipped with an identical sensor payload to enable comparative analysis. A particular emphasis will be placed on evaluating the effects of the (higher) relative velocities between UAVs and manned aircraft.

7. ACKNOWLEDGEMENTS

The project has received funding from the mFUND program of the German Federal Ministry for Transport (BMV). The authors further acknowledge the valuable contributions of Anagha Anand, Leon Alexander Albrecht, Tim Bähr, Vasantha Muruganantham, and Robert Kemmerling to the preparation, execution, and analysis of the flight test, as well as the assistance provided by the numerous volunteers who supported activities on the flight test day.

Contact address:

frickenstein@tu-berlin.de

References

[1] Fabian Frickenstein, Benjamin Lochow, Tom Piechotta, Markus Rossol, Chris Janke, and Maarten Uijt De Haag. Managing Separation Assurance through U-Space Flight Test Results using UAVs and Small Aircraft. In *2025 AIAA DATC/IEEE 44th Digital Avionics Systems Conference (DASC)*, pages 1–10. IEEE, 2025. ISBN: 979-8-3315-2519-4. DOI: 10.1109/DASC66011.2025.11257405.

[2] European Comission. Commission Implementing Regulation (EU) 2021/664 of 22 April 2021 on a regulatory framework for the U-space. *Official Journal of the European Union*, L 139/161, Apr. 2021.

[3] European Comission. Commission Implementing Regulation (EU) 2023/1770 of 12 September 2023 laying down provisions on aircraft equipment required for the use of the Single European Sky airspace and operating rules related to the use of the Single European Sky airspace and repealing Regulation (EC) No 29/2009 and Implementing Regulations (EU) No 1206/2011, (EU) No 1207/2011 and (EU) No 1079/2012. *Official Journal of the European Union*, (L 228/39), Sept. 2023.

[4] Inc. RTCA. DO-260B: Minimum Operational Performance Standards for 1090 MHz Extended Squitter Automatic Dependent Surveillance Broadcast (ADS-B) and Traffic Information Services – Broadcast (TISB), Dec. 2009.

[5] EASA. Technical Specification for ADS-L transmissions using SRD-860 frequency band. ED Decision 2022/024/R Issue 1, EASA, 2022.

[6] EASA. Technical Specification for ADS-L transmissions using SRD-860 frequency band. ED Decision 2022/024/R Issue 2, EASA, 2025.

[7] Pengfei Duan and M. U. De Haag. Transmitting raw GNSS measurements as part of ADS-B: Why, how, and flight test results. In *2012 IEEE/AIAA 31st Digital Avionics Systems Conference (DASC)*, pages 5C1–1–5C1–13. IEEE, 2012. ISBN: 978-1-4673-1700-9 978-1-4673-1699-6 978-1-4673-1698-9. DOI: 10.1109/DASC.2012.6382365.

[8] Benjamin Lochow, Luisa Tautz, and Maarten Uijt de Haag. Enhancing Separation Assurance by Using Newly Developed ADS-L Messages Containing GNSS Raw Measurement Data. 2024.

[9] Bundesministerium für Verkehr. Skalierbare Drohnen-Kommunikationssysteme für U-Space-Gebiete - SKADRO. https://www.bmv.de/SharedDocs/DE/Artikel/DG/mfund-projekte/skadro.html.

[10] Septentrio. Mosaic-X5 Reference Guide, Applicable to version 4.1.4.4 of the Firmware.

[11] Benjamin Lochow, Fabian Frickenstein, Robert Kemmerling, and Maarten Uijt De Haag. Advancing ADS-L: Implementation, Performance Evaluation, and Conformance Monitoring in U-Space. In *2025 AIAA DATC/IEEE 44th Digital Avionics Systems Conference (DASC)*, pages 1–8. IEEE. ISBN: 979-8-3315-2519-4. DOI: 10.1109/DASC66011.2025.11257291.